Extended Abstracts of the 2011 International Conference on Solid State Devices and Materials, Nagoya, 2011, pp1051-1052

G-3-4L

Investigation of Subthreshold Drain Current Mismatch Characteristics for Nanoscale MOSFETs

Jack J.-Y. Kuo and Pin Su
Department of Electronics Engineering & Institute of Electronics, National Chiao Tung University, Hsinchu, Taiwan

ABSTRACT

Subthreshold drain current mismatch characteristics for nanoscale MOSFETs are investigated. To model the subthreshold drain current mismatch more physically and accurately, our study suggests the constant-current method instead of the maximum slope method should be used for the determination of threshold voltage. Our study indicates that the subthreshold swing mismatch is important for devices with small geometries. It is also found that the correlation between the threshold voltage mismatch and the subthreshold swing mismatch needs to be considered in the subthreshold drain current mismatch modeling especially for long channel devices.

INTRODUCTION

Random mismatch is one major problem that hinders the robustness of ultralow-power subthreshold circuits. In this paper, through a comprehensive model-data comparison, the subthreshold drain current mismatch model characteristics of nanoscale MOSFETs are examined and analyzed.

DEVICES AND EXPERIMENTAL

Nanoscale PMOSFETs [1] are investigated in this study. The device used in this study has channel length (L) and width (W) ranging from 54nm to 1um and 0.12um to 5um, respectively. The mismatching properties were measured from identical devices in a matching pair configuration on 60 dies. Statistics on the mismatch in drain current ($\Delta\log(I_d)$), threshold voltage (ΔV_{th}), and subthreshold swing (ΔS) in linear and saturation regions were analyzed.

RESULTS AND DISCUSSION

A. Subthreshold drain current mismatch modeling

The variance of subthreshold drain current mismatch can be expressed as [2]:

$$\sigma^2(\Delta\log(I_d)) = \frac{1}{S^2}\sigma^2(\Delta V_{th}) + \left(\frac{V_{gs}-V_{th}}{S^2}\right)^2\sigma^2(\Delta S) + 2\frac{(V_{gs}-V_{th})}{S^3}\sigma(\Delta V_{th})\sigma(\Delta S)\rho(\Delta V_{th},\Delta S), \quad (1)$$

where S and V_{th} denote the subthreshold swing and threshold voltage, respectively. The RHS of Eq. (1) indicates three components of the subthreshold drain current mismatch, which account for the threshold voltage mismatch ($\sigma(\Delta V_{th})$), subthreshold swing mismatch ($\sigma(\Delta S)$), and the correlation between $\sigma(\Delta V_{th})$ and $\sigma(\Delta S)$ ($\rho(\Delta V_{th}, \Delta S)$) , respectively.

Fig. 1 (a) and (b) compare Eq. (1) with V_{th} determined by the constant-current method ($V_{th}=V_{gs}$ at $I_d= I_0\cdot W/L$ with I_0= 40nA) and the maximum slope method, respectively. It can be seen that the accuracy between data and model is fairly good for both methods at $|V_{gst}|>0$. In the subthreshold regime ($|V_{gst}|<0$), however, the constant-current method shows better accuracy than the maximum slope method. The discrepancy between data and model shown in **Fig. 1**(b) results from the larger $\sigma(\Delta V_{th})$ determined by the maximum slope method.

As shown in **Fig. 2**, the $\sigma(\Delta V_{th})$ determined by the maximum slope method is larger than that determined by the constant-current method. It is believed that the mobility degradation and the source/drain parasitic resistance are taken into account when determining V_{th} by the maximum slope method [3]. Therefore, in order to model the subthreshold drain current mismatch more physically and accurately, the constant-current method is suggested. **Fig. 3** shows fairly good subthreshold drain current mismatch modeling in linear region ($|V_{ds}|$=0.05V) and saturation region ($|V_{ds}|$=1V).

B. Subthreshold swing mismatch

Fig. 4 (a) and (b) show the Pelgrom plot of $\sigma(\Delta V_{th})$ and $\sigma(\Delta S)$, respectively. It can be seen that both the $\sigma(\Delta V_{th})$ and $\sigma(\Delta S)$ increase linearly with $(WL)^{-1/2}$ indicating the random-dopant-fluctuations (RDF) origin [4]. Furthermore, the linear relationship between $\sigma(\Delta S)$ and $(WL)^{-1/2}$ indicates that the $\sigma(\Delta S)$ can be suppressed by adopting larger W devices. This channel-width dependence of $\sigma(\Delta S)$ for planar bulk devices is different from that present in lightly doped FinFET devices, which shows weak channel-width dependence for $\sigma(\Delta S)$ [5]. The difference stems from the fact that the $\sigma(\Delta S)$ is RDF origin for planar bulk devices, while the $\sigma(\Delta S)$ is line edge roughness (LER) origin for lightly doped FinFET devices.

C. Relevance of correlation $\rho(\Delta V_{th}, \Delta S)$

Fig. 5 (a) and (b) show the data-model comparison with and without the consideration of $\rho(\Delta V_{th}, \Delta S)$. It can be seen that the data-model shows discrepancy for long channel devices when $\rho(\Delta V_{th}, \Delta S)$ is not considered. This is because the ΔV_{th} and ΔS are strongly correlated for long channel devices, as shown in **Fig. 6**. In addition, **Fig. 6** shows that the $\rho(\Delta V_{th}, \Delta S)$ decreases with channel length. For long channel devices, the $\rho(\Delta V_{th}, \Delta S)$ is high because the channel dopant increases V_{th} and S simultaneously. But for short channel devices, the S increases while the V_{th} decreases due to short channel effects and results in a smaller $\rho(\Delta V_{th}, \Delta S)$.

Fig. 7 compares the mismatch signature [6] in terms of the autocorrelation coefficient for devices with various channel length in the subthreshold region. The autocorrelation coefficient is an index showing the dominance of ΔV_{th} on the drain current mismatch. It can be seen that the autocorrelation coefficient decreases with downscaling L for a given $|V_{gst}|$ due to short channel effects.

ACKNOWLEDGEMENTS

This work was supported in part by the National Science Council of Taiwan under Contract NSC99-2221-E-009-174, and in part by the Ministry of Education in Taiwan under ATU Program.

REFERENCES

[1] J. J.-Y. Kuo *et al.*, *IEEE Trans. Electron Dev.*, p.284, 2009.
[2] P. Magnone *et al.*, *IEEE Trans. Electron Dev.*, p. 2848, 2010.
[3] A. Oritiz-Conde *et al.*, *Microelectron. Reliab.*, p.583, 2002.
[4] T. Mizuno *et al.*, *IEEE Trans. Electron Dev.*, p. 2216, 1994.
[5] C.-H. Lin *et al.*, *VLSI Symp. Tech. Dig.* p.16, 2011.
[6] P. Andricciola *et al.*, *IEDM Tech. Dig.*, p.711, 2009.

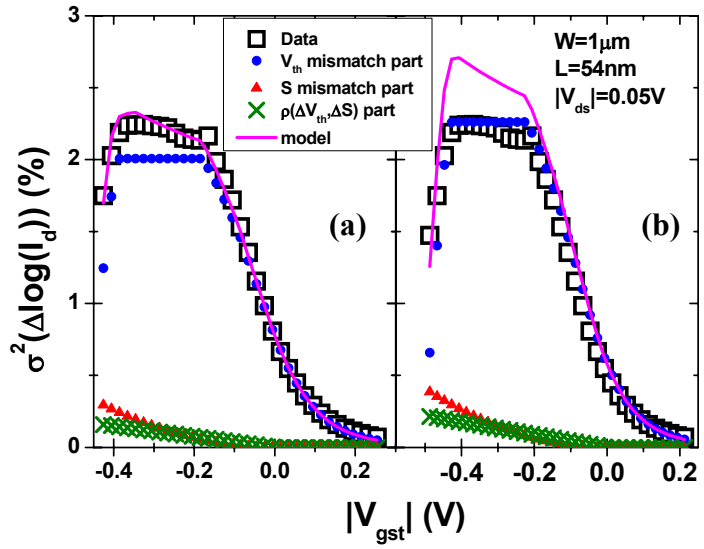

Fig. 1 Data-model comparison with the V_{th} determined by (a) the constant-current method and (b) the maximum slope method.

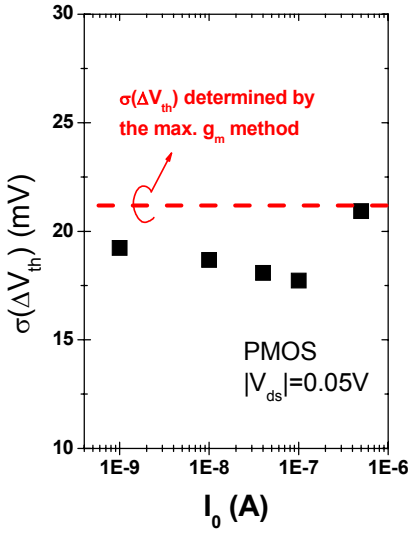

Fig. 2 Comparison of the $\sigma(\Delta V_{th})$ determined by the maximum slope method and the constant-current method with various I_0.

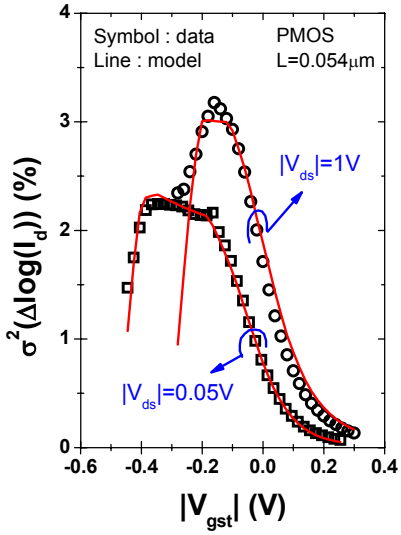

Fig. 3 Data-model comparison at $|V_{ds}|$=0.05V and 1V using the constant-current method.

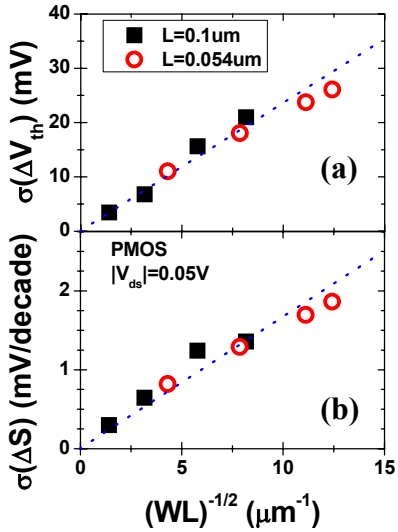

Fig. 4 Pelgrom plot of (a) $\sigma(\Delta V_{th})$ and (b) $\sigma(\Delta S)$.

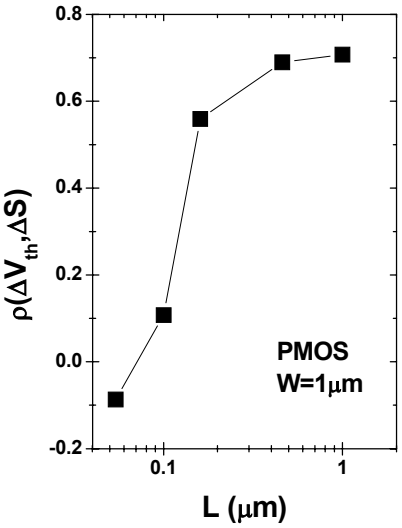

Fig. 6 ΔV_{th} and ΔS are strong correlated for long channel devices.

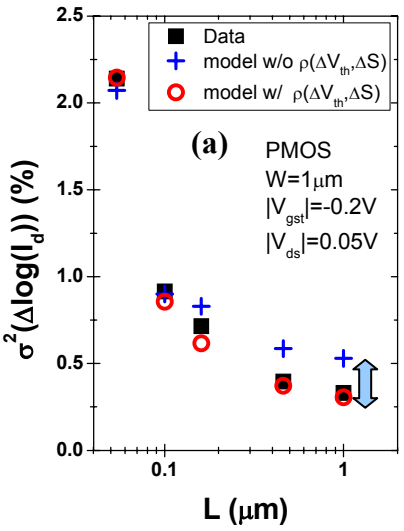

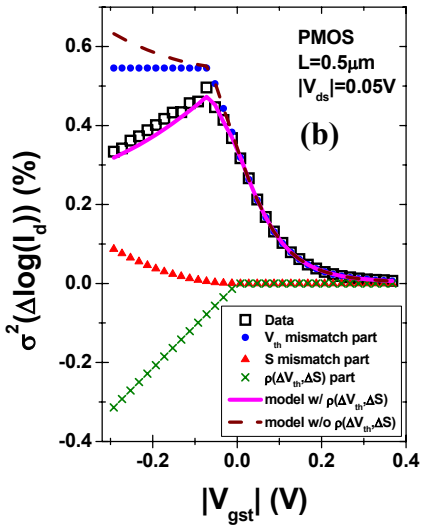

Fig. 5 (a) Data-model comparison with and without the consideration of $\rho(\Delta V_{th}, \Delta S)$. (b) The $\rho(\Delta V_{th}, \Delta S)$ component is especially important for long channel devices. The model overestimates the mismatch without considering $\rho(\Delta V_{th}, \Delta S)$.

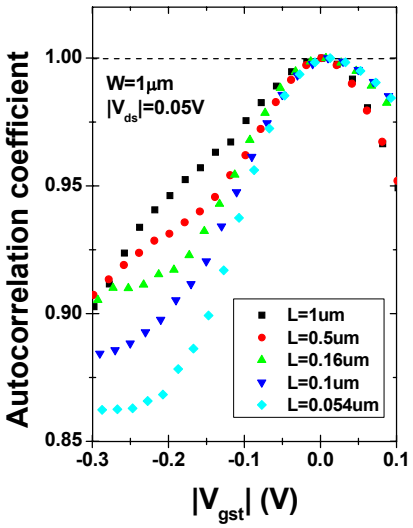

Fig. 7 For a given $|V_{gst}|$, the autocorrelation coefficient decreases with downscaling L in the subthreshold region.